physica status solidi
pss
www.pss-journals.com

reprint

WILEY-VCH

Phys. Status Solidi B **252**, No. 1, 219–229 (2015) / **DOI** 10.1002/pssb.201451202

physica status solidi b
www.pss-b.com
basic solid state physics

The effect of surface roughness and grain-boundary scattering on the electrical conductivity of thin metallic wires

Luis Moraga*[,1], Claudio Arenas[2,3], Ricardo Henriquez[4], and Basilio Solis[1]

[1] Departamento de Ciencias Básicas, Facultad de Ingeniería, Universidad Central de Chile, Santa Isabel 1186, Santiago 8330601, Chile
[2] Departamento de Física, Facultad de Ciencias Físicas y Matemáticas, Universidad de Chile, Blanco Encalada 2008, Casilla 487-3, Santiago 8370449, Chile
[3] Synopsys, Inc. Avenida Vitacura 5250, Oficina 708, Vitacura, Santiago, Chile
[4] Departamento de Física, Universidad Técnica Federico Santa Maria, Avenida España 1680, Valparaíso, Chile

Received 16 April 2014, revised 25 June 2014, accepted 14 July 2014
Published online 27 August 2014

Keywords electrical conductivity, grain boundaries, surface roughness, thin metallic wires

* Corresponding author: e-mail luismoragajaramillo@gmail.com, Phone: +(56-2) 25826968, Fax: +(56-2)25826927

We report a new formula for the electrical conductivity of a thin wire of rectangular cross-section, obtained from an exact solution of the Boltzmann equation by assuming perfectly diffuse surface scattering and absence of grain boundaries. Also, we calculate the electrical conductivity of polycrystalline metallic wires, both for the case of rectangular and circular cross-sections and for arbitrary values of Fuchs' specularity parameter, by means of a seminumerical procedure that solves the Boltzmann equation by summing over classical trajectories in accordance with Chambers' method. Following Szczyrbowski and Schmalzbauer, the scattering by grain boundaries is represented by a peculiar specularity parameter and a boundary transmittance. The difference between one and the sum of these two probabilities measures the probability of diffuse scattering. We examine the dependence of the conductivity on the values of these parameters and the effects of disorder on the diameters of the grains.

1 Introduction Contemporary advances in computer technology have required increasing the density of memory and logical circuits. This trend has been possible only at the cost of diminishing the physical dimensions of the metallic interconnects. However, it has been found that, when the thickness of a wire is comparable to the mean free path of the conduction electrons, its electrical resistivity increases considerably. This results, in turn, in a corresponding augmentation of the thermal dissipation and a propagation delay in the microcircuit. The effect is complicated by the added contribution of grain-boundary scattering that seems to be an undesirable result of the majority of the known fabrication procedures [1–5].

The obvious technological importance of these facts has led to a number of experimental studies on the conductivity of metallic wires. Unfortunately, the wealth of new data obtained in this way has not been accompanied by corresponding theoretical progress. In order that decisive advances are possible it is necessary to find quantitative theories, firmly based on fundamental principles, that allows the experimenter both to explain the phenomena and to predict others. It would be useful, for instance, to have a solution of the Boltzmann transport equation describing the electron's distribution function under the combined effects of external fields, distributed imperfections, rough external surfaces, and those of grain boundaries [6]. Alternatively, it would be equally convenient to have Green's functions describing, with enough realism, the behavior of such materials [7, 8]. Unfortunately, it seems that the totality of fundamental results known until now can provide only partial answers to the many questions found in practice. Also, these are more than half a century old. The electrical conductivity of a thin wire of circular cross-section was calculated by Dingle [9]. The corresponding result for wires of square cross-section was obtained by MacDonald and Sarginson [10] for the special case of completely diffuse surface scattering. Both theories were published in 1950. (The relevant experimental work up to 1980 has been reviewed by Sambles et al. [11].)

At the present, the most successful treatment of these effects is the theory of Mayadas et al. [13]. For instance, if σ_g and σ_0 denote the conductivities of bulk samples with and without grain boundaries,

$$\frac{\sigma_g}{\sigma_0} = 3\left[\frac{1}{3} - \frac{\alpha}{2} + \alpha^2 - \alpha^3 \ln\left(1 + \frac{1}{\alpha}\right)\right], \tag{1}$$

where $\alpha = \lambda R/(D(1-R))$, λ is the bulk value of the mean free path of the conduction electrons and D is the average diameter of the grains (or the average distance between grain boundaries). Here (and hereafter), R denotes the reflectance of an individual grain boundary. In this paper, Mayadas and Shatzkes also found a formula for the case of a thin film [13]. Finally, we note that Dimmich and Warkusz have developed an extension of Mayadas and Shatzkes' work appropriate for wires of circular cross-section [15].

However, Szczyrbowski and Schmalzbauer have noted that, since Mayadas and Shatzkes' theory relies on a first-order perturbative procedure, the resulting formulae should be valid only for high enough values of the barrier transmittance T – or low enough values of the barrier reflectance R [14].

In this paper, we report results of two different kinds. First, we derive in detail a new formula giving the electrical conductivity of a thin wire of rectangular cross-section, bounded by rough surfaces, and in the absence of grain boundaries. The formula is our Eq. (2). The solution for a wire of square cross-section has already been found by McDonald and Sarginson [10]; while the corresponding formula for wires of circular cross-section has been published by Dingle [9]. The fact that the Boltzmann transport equation has not been solved for cases more complicated – and also more interesting – than these (such as, for instance, thin wires of rectangular cross-section with $p \neq 0$, or wires bounded by rough surfaces and crossed by grain boundaries) has not been caused inadvertently but because these solutions simply do not exist in this semiclassical context. As we show in this paper, the solutions that intend to represent these cases contain functions that are continuous but that have derivatives that are discontinuous at almost every point.

The second kind of result is based on the application of the method of characteristics curves (or Chambers' method) for solving the Boltzmann transport equation [16, 17]. The characteristic function, determining the solution of the transport equation appropriate for a particular case, can be written as a sum over all possible classical trajectories of a carrier traversing the material. For a given point in the material and a given terminal velocity, the number of these trajectories is often countable infinite. If the sum is performed over all these trajectories, we obtain the exact solution. The method we propose here consists in performing the sum over a random sample that is finite; but that contains enough trajectories so that the sample is representative with the required accuracy. (This means, depending on the case, to perform the sum over 50–500 classical trajectories per point.) In this way, we can calculate approximately the transport properties of systems with varying complexities. Thus, we present in this paper quantitative estimates of the effect on the electrical conductivity of thin wires with different amounts of surface diffusiveness, of values of transmissibility (or of reflectivity) of grain boundaries, or having different degrees of disorder and the net effect of changing the different linear dimensions in units of the mean free path.

Finally, we apply the theory developed in this paper to a tentative analysis of the measurements of Steinhögl et al. [1] of thin copper wires and those of Josell et al. of thin silver wires [2].

2 Exact results

In this section, we report a formula describing the electrical conductivity σ of a thin wire of rectangular cross-section, obtained from an exact solution of the Boltzmann transport equation (4) in the case of perfectly diffuse surface scattering ($p = 0$) and in the absence of grain-boundary scattering. The formula is:

$$\begin{aligned}\frac{\sigma}{\sigma_0} = {} & 1 - \frac{3\lambda}{8}\left(\frac{1}{D_x} + \frac{1}{D_y}\right) + \frac{4\lambda^2}{5\pi D_x D_y} \\ & - \frac{6\lambda}{\pi}\int_0^{\pi/2} \mathrm{d}\theta \cos^2\theta \sin^2\theta \\ & \times \left\{\int_0^{\phi_c} \mathrm{d}\phi \exp\left(-\frac{D_x}{\lambda \sin\theta\cos\phi}\right)\right. \\ & \times \left(-\frac{\cos\phi}{D_x} + \frac{\sin\phi}{D_y} + 2\lambda\frac{\cos\phi}{D_x}\frac{\sin\phi}{D_y}\sin\theta\right) \\ & + \int_0^{\pi/2-\phi_c} \mathrm{d}\phi \exp\left(-\frac{D_y}{\lambda\sin\theta\cos\phi}\right) \\ & \times \left.\left(\frac{\sin\phi}{D_x} - \frac{\cos\phi}{D_y} + 2\lambda\frac{\cos\phi}{D_x}\frac{\sin\phi}{D_y}\sin\theta\right)\right\},\end{aligned} \tag{2}$$

where σ_0 is the conductivity of the bulk, $\phi_c = \arctan\mu$ and $\mu = D_y/D_x$ is the aspect ratio. (Without losing generality, we can assume that $\mu \leq 1$.) A detailed derivation of this formula is presented in Appendix A.

On the other hand, it can be shown that no exact solution of the Boltzmann transport equation is possible in the partially diffuse case $p \neq 0$. We offer a proof of this in Appendix B.

In Fig. 1, we plot the values of the electrical resistivity of a thin wire of rectangular cross-section, calculated from this formula as a function of D_y/λ, for different values of the aspect ratio. It is seen that it coincides with the MacDonald and Sarginson result in the case $D_x = D_y$ and with Fuch's expression for a thin film of thickness D_y in the opposite case $D_x \gg D_y$ [10, 12].

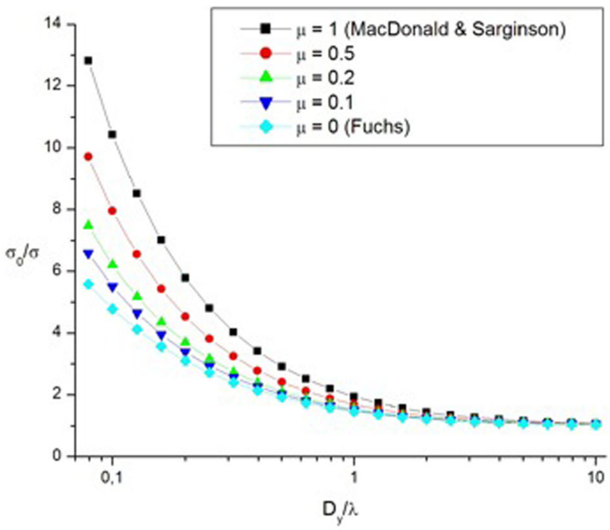

Figure 1 Effect of the aspect ratio on the electrical resistivity of a thin wire of rectangular cross-section. $\mu = D_y/D_x$ denotes the aspect ratio.

3 Chambers' method

All theoretical results reported here are based on the Boltzmann transport equation [18]

$$-\frac{e}{m}\mathbf{E}\cdot\frac{\partial f}{\partial \mathbf{v}}+\mathbf{v}\cdot\frac{\partial f}{\partial \mathbf{r}}=-\frac{1}{\tau}(f-f_0), \tag{3}$$

assuming valid the relaxation-time approximation. Here, $f_0=\{\exp[(\mathcal{E}-\mu)/k_{\mathrm{B}}T]+1\}^{-1}$ is the distribution at thermodynamic equilibrium (Fermi–Dirac distribution). As we are interested in the conductivity, we assume further the validity of Ohm's law. Thus, the out-of-equilibrium part of the distribution $f_1=f-f_0$ is determined by

$$\mathbf{v}\cdot\frac{\partial f_1}{\partial \mathbf{r}}+\frac{f_1}{\tau}=-e(\mathbf{E}\cdot\mathbf{v})\left(-\frac{\partial f_0}{\partial \mathcal{E}}\right). \tag{4}$$

Heretofore, it has not been possible to obtain a solution of this equation that takes into account the combined effects of distributed impurities, surface roughness, and grain-boundary scattering. However, the method of characteristics seems to offer a promising route for developing a useful seminumerical procedure that allows to do all this [17]. In the present context, the method has been developed by Chambers [16] and has been successfully applied to the solution of a number of interesting problems.

The method consists in this: The *characteristics* are the curves $\mathbf{r}(t)$, $\mathbf{v}(t)$ – depending on parameter t – that (in this case) are solutions of the differential equations

$$\frac{\mathrm{d}\mathbf{v}}{\mathrm{d}t}=\frac{1}{m}\mathbf{F};\quad \frac{\mathrm{d}\mathbf{r}}{\mathrm{d}t}=\mathbf{v}, \tag{5}$$

where $\mathbf{F}$ is the total force acting on the particle.

Assuming that these curves exist and are real we note that, along a given characteristic, Eq. (4) transforms into

$$\frac{\mathrm{d}f_1}{\mathrm{d}t}+\frac{f_1}{\tau}=-e(\mathbf{E}\cdot\mathbf{v})\left(-\frac{\partial f_0}{\partial \mathcal{E}}\right). \tag{6}$$

Thus, a partial differential equation is reduced to an ordinary differential equation. The physical interpretation of this procedure is that the value of f_1, specified initially at $t=t_0$, is transmitted along the characteristic and determines the value of this function at the required point $\mathbf{r}(t)$, $\mathbf{v}(t)$.

In the case of the Boltzmann transport equation, these characteristics always exist because they coincide with the classical trajectories. Furthermore, the corresponding ordinary differential equation is of the first order and, thus, can always be solved by quadrature. In the simplest case defined by Eq. (6), the solution is

$$f_1=-e\tau(\mathbf{E}\cdot\mathbf{v})\left(-\frac{\partial f_0}{\partial \mathcal{E}}\right)\left(1-Fe^{-t/\tau}\right), \tag{7}$$

where F is an arbitrary function to be determined by the boundary conditions, and t can be interpreted as the time spent by the particle, flying along the classical trajectory, as it moves between successive interactions with the boundaries. We describe now how these quantities are computed.

The effects of external fields and that of distributed impurities appear explicitly in the Boltzmann equation, but the consequences of surface roughness or grain-boundary scattering operate through the boundary conditions. According to Chambers, these boundary conditions determine the function $Fe^{-t/\tau}$ in Eq. (7) as follows:

(i) Given a point $\mathbf{r}$ inside the material and a possible velocity $\mathbf{v}$, the value of function $Fe^{-t/\tau}$ is obtained by performing a sum over all contributions from the classical trajectories that end at $\mathbf{r}$, moving in the direction $\mathbf{v}$, and starting either at one of the rough surfaces bounding the sample or at one of the grain boundaries. Each trajectory may execute any number of specular reflections at these boundaries or traverse, without changing its direction, any number of grain boundaries. Given one of these trajectories, t is the net time spent performing the classical movement from this initial to the given final point.

(A particle is specularly reflected at a given surface if the angle of incidence of its trajectory equals the angle of reflection; i.e. the tangential component of its velocity remains unchanged while its normal component is reversed.)

(ii) The effect of surface roughness is described by a specularity parameter p, which is a number between zero and one [19]. The specularity parameter measures the probability that the carrier is specularly reflected at the given surface, while the balance $q=1-p$ describes the probability that the scattering is completely diffuse and the particle is thereafter lost to the conduction process.

(iii) Szczyrbowski and Schmalzbauer have extended Chambers' method in order to include the effects on the electrical conductivity arising from grain-boundary scattering in

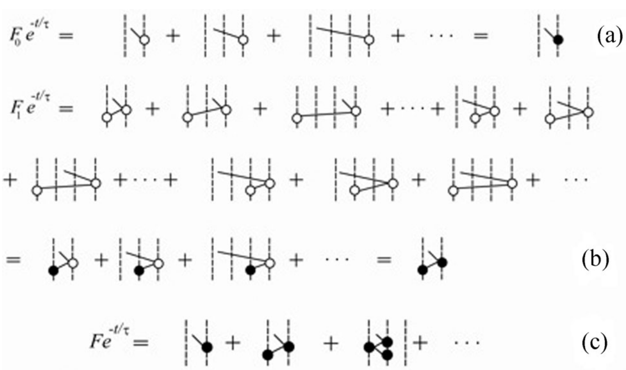

Figure 2 Diagrammatical calculation of the characteristic function of a periodic array of scattering planes. (a), (b), (c) represent Eqs. (9), (11) and (13) of the text, respectively. Circles with an empty interior denote reflectivity parameters. Black circles denote the same parameters but modified (or renormalized) by repeated transmissions through other planes.

polycrystalline samples [14]. In this treatment, the scattering properties of a grain boundary are characterized by two parameters, a specularity parameter $p_{\rm GB}$ and a transmittance $T_{\rm GB}$. As before, the reflectivity $p_{\rm GB}$ measures the probability that an incoming carrier is specularly reflected at the given grain boundary, while $T_{\rm GB}$ describe the probability that it can traverse the boundary without modifying its trajectory. The remaining probability $q_{\rm GB} = 1 - T_{\rm GB} - p_{\rm GB}$ describes the carriers that are diffusely scattered at the boundary and are subtracted from the out-of-equilibrium distribution function. It is supposed that $p_{\rm GB}$, $q_{\rm GB}$, and $Tp_{\rm GB}$ are numbers between zero and one and have, as a first approximation, the same value for all grain boundaries of the sample.

The simplest possible model for the distribution of grain boundaries in a real sample consist in representing them by a set of parallel planes (and parallel, say, to the x–y plane) located at random points $z_1, z_2, \cdots, z_{N+1}$ [13]. The set of distances $D_i = z_{i+1} - z_i$ between these planes can be assumed to be a random variate, obeying a definite probability distribution.

It is interesting to note that, when the grain boundaries modeled in this way are equidistant $D = D_i$ (that is, there is no disorder), extend indefinitely in the x–y direction, and the movement is such that the component v_z of the velocity remains constant (that is, in the presence of an electric, but not of a transverse magnetic field) the sum over trajectories prescribed by Szczyrbowski and Schmalzbauer may be performed by hand. Thus, if $F^+e^{-t/\tau}$ denotes the branch of $Fe^{-t/\tau}$ in the case $v_z > 0$ and $0 \leq z \leq D$, it is easy to see that

$$F^+e^{-t/\tau} = \frac{q_{\rm GB}e^{-z/\tau v_z}}{1-(T_{\rm GB}+p_{\rm GB})e^{-D/\tau v_z}}. \tag{8}$$

The remaining branch $F^-e^{-t/\tau}$, describing the case $v_z < 0$, is obtained from this formula by replacing z by $D - z$ and v_z by $|v_z|$. We can show this as follows (Fig. 2). Let us consider first the sum $F_0e^{-t/\tau}$ of all trajectories ending at z with velocity v_z, starting from some grain boundary and eventually traversing other grain boundaries but without suffering any reflection along its way. Clearly, this is given by

$$\begin{aligned} F_0e^{-t/\tau} &= q_{\rm GB}e^{-z/\tau v_z} + q_{\rm GB}T_{\rm GB}e^{-(z+D)/\tau v_z} \\ &\quad + q_{\rm GB}T_{\rm GB}^2e^{-(z+2D)/\tau v_z} \\ &\quad + q_{\rm GB}T_{\rm GB}^3e^{-(z+3D)/\tau v_z} \\ &\quad + \cdots \\ &= \frac{q_{\rm GB}e^{-z/\tau v_x}}{1-T_{\rm GB}e^{-D/\tau v_z}} = Q_{\rm GB}e^{-z/\tau v_x}; \end{aligned} \tag{9}$$

if we define the effective (or renormalized) parameters $P_{\rm GB}$ and $Q_{\rm GB}$; that is, the true (or bare) parameters $p_{\rm GB}$ and $q_{\rm GB}$ modified by multiple transmissions through other grain boundaries,

$$P_{\rm GB} = \frac{p_{\rm GB}}{1-T_{\rm GB}e^{-D/\tau v_z}}; \quad Q_{\rm GB} = \frac{q_{\rm GB}}{1-T_{\rm GB}e^{-D/\tau v_z}}. \tag{10}$$

In Fig. 2, this process is symbolized by replacing a circle with empty interior with a black circle.

Let us consider now the sum over all trajectories that have suffered exactly one reflection along its way. Excluding the segments already summed in Eq. (9), this is

$$\begin{aligned} F_1e^{-t/\tau} &= \sum_{n=1}^{\infty}\sum_{m=0}^{\infty} q_{\rm GB}T_{\rm GB}^{n+m-1}p_{\rm GB}e^{-[z+(n+m)D]/\tau v_z} \\ &= \sum_{n=1}^{\infty}\frac{q_{\rm GB}p_{\rm GB}T_{\rm GB}^{n-1}e^{-(z+nD)/\tau v_z}}{1-T_{\rm GB}e^{-D/\tau v_z}} \\ &= \frac{q_{\rm GB}p_{\rm GB}e^{-(z+D)/\tau v_z}}{(1-T_{\rm GB}e^{-D/\tau v_z})^2} \\ &= Q_{\rm GB}P_{\rm GB}e^{-(z+D)/\tau v_z}. \end{aligned} \tag{11}$$

In the same way, the sum over all trajectories that have suffered *two* reflections (excluding those contributions already summed) is

$$\begin{aligned} F_2e^{-t/\tau} &= Q_{\rm GB}P_{\rm GB}^2e^{-(z+2D)/\tau v_z} \\ &= \frac{q_{\rm GB}p_{\rm GB}^2e^{-(z+2D)/\tau v_z}}{(1-T_{\rm GB}e^{-D/\tau v_z})^3}. \end{aligned} \tag{12}$$

Thus, the total sum over all trajectories is

$$\begin{aligned} &F^+e^{-t/\tau} \\ &= \sum_{n=0}^{\infty} F_ne^{-t/\tau} \\ &= Q_{\rm GB}e^{-z/\tau v_x}\sum_{n=0}^{\infty} P_{\rm GB}^ne^{-nD/\tau v_z} \\ &= \frac{Q_{\rm GB}e^{-z/\tau v_z}}{1-P_{\rm GB}e^{-D/\tau v_z}} \\ &= \frac{q_{\rm GB}e^{-x/\tau v_z}}{1-T_{\rm GB}e^{-D/\tau v_z}}\left[\frac{1}{1-p_{\rm GB}e^{-D/\tau v_z}/(1-T_{\rm GB}e^{-D/\tau v_z})}\right]; \end{aligned} \tag{13}$$

which is exactly result (8). The seminumerical procedure, to be described presently, confirms this result.

Mayadas and Shatzkes further considered the possibility of having disorder, in the form of a Gaussian distribution of grain diameters with mean D and standard deviation s

$$e(D_1, \cdots, D_N) = (2\pi s^2)^{-N/2} \exp\left[-\sum_{i=1}^{N} \frac{(D_i - D)^2}{2s^2}\right]. \quad (14)$$

On the other hand, measurements of grain diameters in actual samples tend to suggest that the the underlying probability distribution is lognormal instead of normal. In the following sections, we study the effects of disorder in some typical cases. We find, in accordance with Mayadas and Shatzkes' theory, that the effects are quite small [13].

4 Conductivity of thin wires In this section, we solve the Boltzmann transport equation by approximating the sum over all classical trajectories, which define the function $Fe^{-t/\tau}$ in Eq. (7), by summing over a finite random sample of these paths. Given a point $\mathbf{r}$ and a velocity $\mathbf{v}$ of a carrier traversing the wire and belonging to the out-of-equilibrium distribution f_1, the computer calculates a possible classical path leading to this point by following its history backwards in time – going through reflections or transmissions at sample surfaces and grain boundaries – until the point where (by chance) the particle has been incorporated into f_1. Then, the total flight time t (in units of the time of relaxation τ) is calculated and the result accumulated in order to build F. The procedure is repeated with other trajectories defined by the same values of $\mathbf{r}$ and $\mathbf{v}$, until sufficient statistics have been accumulated. Later on, an integration over all possible values of $\mathbf{r}$ and $\mathbf{v}$ is performed and the current and, hence the electrical conductivity, is obtained.

The trajectories (and flight times) are not calculated by following in detail the path of each particle. Instead, the computer determines the sequence of critical points; i.e., a possible point of intersection of the path with one of the surfaces of the sample or a grain boundary. For instance, if a particle happens to be at a point of coordinates x, y, and z inside a wire of rectangular cross-section, extending from $0 \le x \le D_x$, $0 \le y \le D_y$, and a grain of diameter D, extending from $0 \le z \le D$, the machine computes the following six time intervals

$$t_1 = -\frac{x}{v_x}; \quad t_2 = \frac{D_x - x}{v_x};$$
$$t_3 = -\frac{y}{v_y}; \quad t_4 = \frac{D_y - y}{v_y};$$
$$t_5 = -\frac{z}{v_x}; \quad t_6 = \frac{D - z}{v_z}. \quad (15)$$

The time interval necessary for reaching the next critical point is the smallest positive value of these six numbers. Let it be t_i. The coordinates x', y', and z' of the critical point are

$$x' = x + v_x t_i; \quad y' = y + v_y t_i; \quad z' = z + v_z t_i. \quad (16)$$

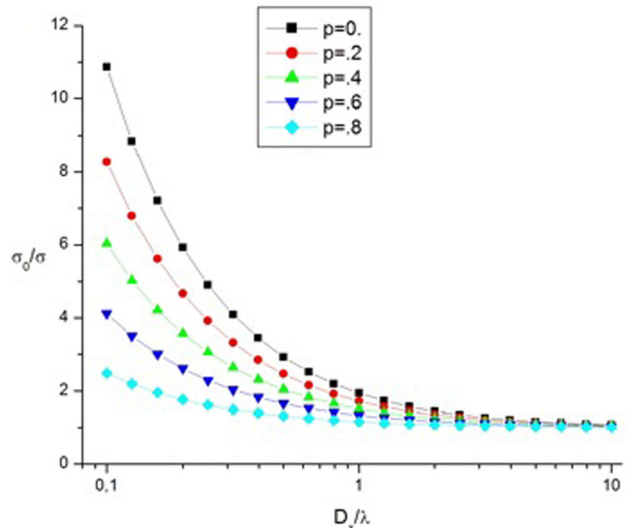

Figure 3 Effects of the surface reflectivity p on the electrical resistivity of a thin wire of square cross-section with side 50 nm in the absence of grain-boundary scattering.

A similar procedure is followed when treating wires of circular cross-section.

The next step depends on the value of a random number generated at this point. If the critical point happens to belong to a sample surface, a fraction p of the trials the particle is specularly reflected (meaning that the sign of the normal component of the velocity is reversed) and the remaining $1 - p$ fraction of the trials the particle is removed – and a new trajectory is initiated. If the critical point happens to be on a grain boundary, a fraction p_{GB} of the trials the particle is reflected, another fraction T_{GB} of the trials the particle is transmitted without change across the boundary and the remaining fraction $1 - p_{GB} - T_{GB}$ of the trials, the particle is removed. The total flight time is accumulated as $t = \sum_i t_i$. When the particle has not been removed, the procedure is iterated by calculating the occurrence of the next critical point.

In order to distinguish the effect of surface scattering from that occurring at the grain boundaries, we examine first the case when the latter is ineffective; that is when $p_{GB} = 0$ and $T_{GB} = 1$. (The analysis of experimental data at the end of this section suggests, however, that, in typical polycrystalline wires, the effect of grain scattering is considerable.) Representative results, where we vary the mean free path on a wire of square cross-section with $D_x = D_y = 50$ nm for different values of the surface reflectivity p, are plotted in Fig. 3. Comparable results in the case of a thin wire of circular cross-section are shown in Fig. 4. (In this case, the results of the seminumerical procedure coincide with those obtained from Dingle's formula [9].) MacDonald and Sarginson noted that the conductivity of a wire of circular cross-section σ_C

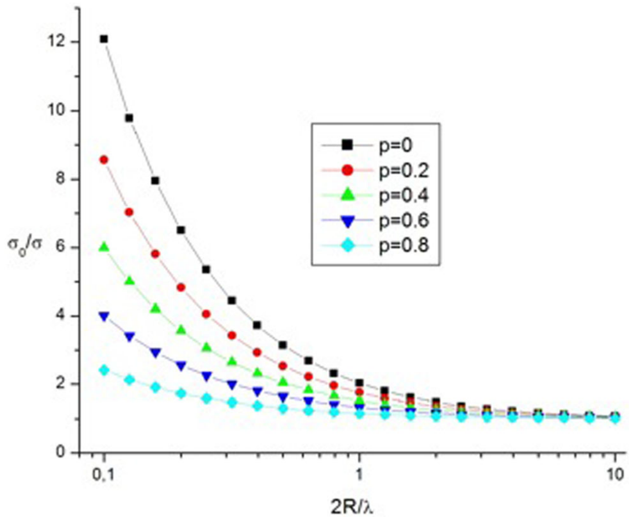

Figure 4 Effect of the surface reflectivity p on the electrical resistivity of a thin wire of circular cross-section. (Dingle's theory [9].)

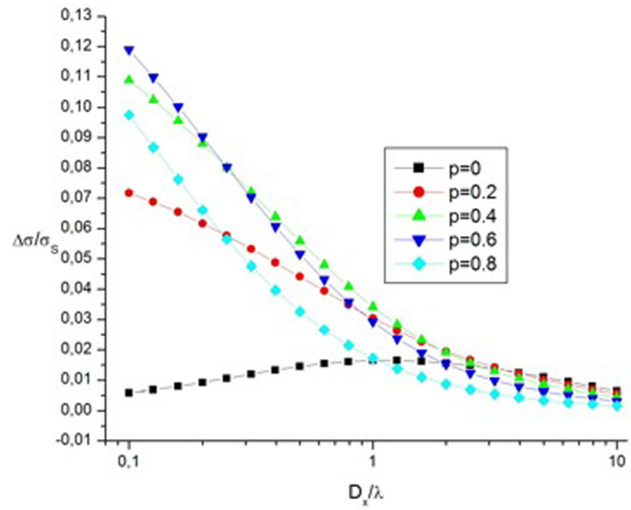

Figure 5 Fractional difference $(\sigma_C - \sigma_S)/\sigma_S$ between the conductivity σ_C of a thin wire of circular cross-section with radius $R = D_x/\sqrt{\pi}$ and the electrical conductivity σ_S of an identical thin wire of square cross-section with sides $D_x = D_y$, for different values of the surface reflectivity p.

is larger than σ_S, the conductivity of an identical wire of square cross-section at equal values of λ in the case $p = 0$, even if one scales the radius R to an effective $D_x = D_y$ by means of $D_x = \sqrt{\pi}R$ [10]. In Fig. 5, we have plotted the fractional change $(\sigma_C - \sigma_S)/\sigma_S$ in the general ($p \neq 0$) case. It is seen that the discrepancies can be as high as 12% at small thicknesses. This adds weight to an observation of Golledge, Preist, and Sambles who pointed out that the most important factor in determining the resistance in such systems is the specific cross-sectional *geometry* of a thin wire. In comparison with this, they concluded, the precise form of the specularity function is largely insignificant. Thus, for instance, it is not permissible to treat approximately a rectangular wire as a wire of circular cross-section. Rather it is necessary, for an adequate theoretical treatment, to model the specific shape of the actual wire under consideration [20].

We model grain boundaries in thin wires as barriers that are plane and parallel, oriented perpendicularly to the axis of the wire and located at the points $z = z_i$. In practice, for wires that are thin enough, the transversal dimensions of the grains have been found to be equal to those of the wire. Also, the distance between adjacent grain boundaries $D_i = z_{i+1} - z_i$ is (roughly) the same as the minimum between the wire's height and width [1, 3]. As noted before, these grain boundaries are described by a reflectivity p_{GB} and a transmissivity T_{GB}. It is supposed that p_{GB}, T_{GB}, and $1 - p_{GB} - T_{GB}$ are numbers between zero and one. Furthermore, we assume that these numbers uniformly describe all grain boundaries.

In Fig. 6, we plot the resistivity of a thin wire of square cross-section, in the extreme rough case $p = p_{GB} = 0$, as a function of the common transmissibility T_{GB} of the grain boundaries. We assume that the distances between grain boundaries are the same for all grains, $D_i = D$; that is, that we have perfect order. We see that the effects of grain-boundary scattering are considerable. The corresponding resistivity of a wire of circular cross-section is shown in Fig. 7.

Furthermore, we investigate the effects of disorder on the resistivity of a thin wire. This is done by assuming a lognormal distribution of grain diameters D_i with mean D and standard deviation s. In Fig. 8, we plot the fractional changes of the wire resistance as a function of the degree of disorder s and the length of the mean free path. It is seen that the effect is small. This accords with Mayadas and Shatzkes' theory, where it was concluded that the effect of s is measured in the scale of the wavelength of the conduction electron (or in the inverse of the Fermi wave vector k_F) as a

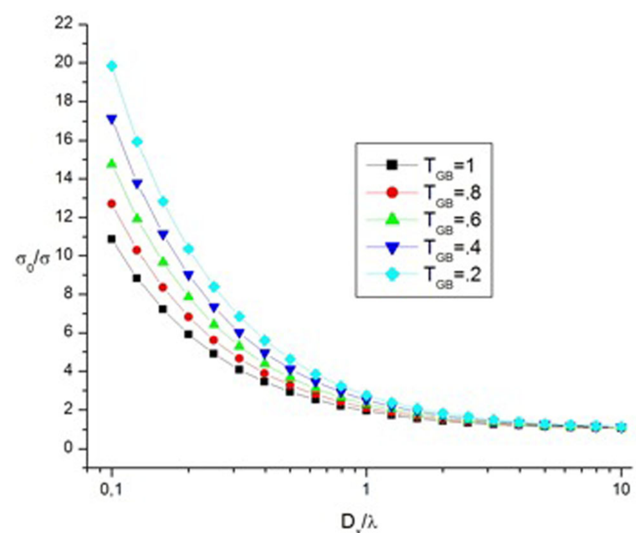

Figure 6 Effect of transmissibility of grain boundaries T_{GB} on the electrical resistivity of thin wires of square cross-section ($D_x = D_y = D = 50$ nm) in the case of completely diffuse scattering $p = p_{GB} = 0$.

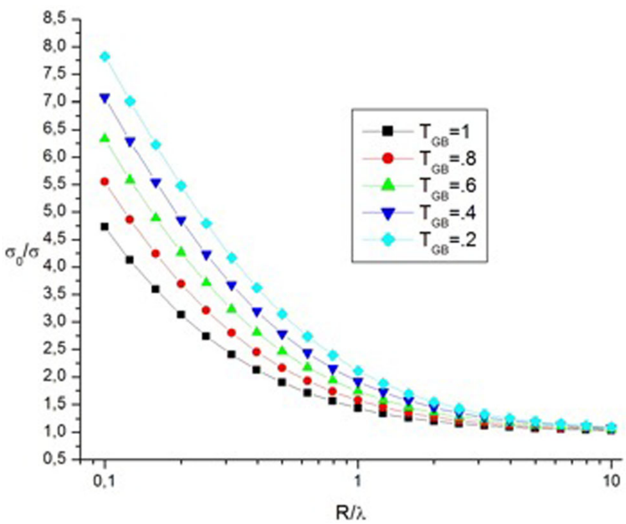

Figure 7 Effect of the transmissibility of grain boundaries T_{GB} on the electrical resistivity of wires of circular cross-section of radius R equal to 50 nm in the case of completely diffuse scattering $p = p_{GB} = 0$.

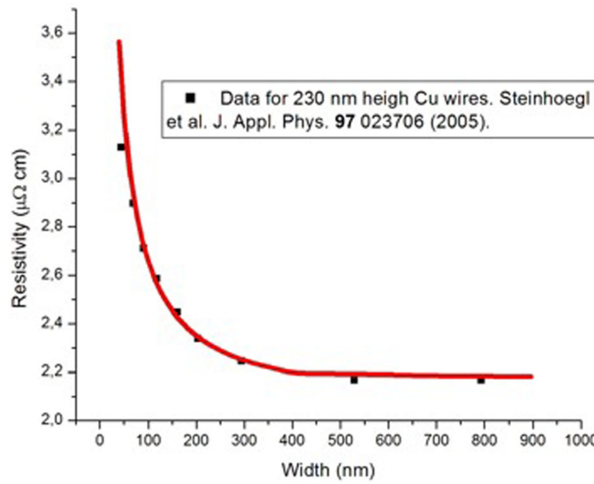

Figure 9 Tentative fit of the theory of this work to data of Steinhögl et al. on the dependence on width of the resistivity of thin Cu wires of rectangular cross-section with height equal to 230 nm. (Fig. 8 of Ref. [1].) $p = 0.9$; $p_{GB} = 0.4$; $T_{GB} = 0.4$; $\rho_0 = 2.0\ \mu\ \Omega$ cm; $\lambda = 150$ nm.

factor of the order $\exp(-k_F^2 s^2)$ – which is negligible for most metals [13].

Finally, we apply the formalism developed here to a tentative interpretation of the electrical conductivity of two recently published measurements on thin wires. The first refers to 230 nm height Cu wires, as reported in Fig. 8 of a paper by Steinhögl et al. [1]. Following these authors, we assume the grain size D to be equal to the wire width if D_x is smaller than 400 nm, and saturates at this value (about twice the height of the wire) if $D_x > 400$ nm; and that that the bulk resistivity $\rho_0 = 2.00\ \mu\ \Omega$ cm. The resulting fit is illustrated in Fig. 9. We find that a satisfactory description can be obtained by assuming a bulk value of the mean free path $\lambda = 150$ nm, that $p = 0.9$, $p_{GB} = 0.4$, and $T_{GB} = 0.4$. In Fig. 10, we plot a corresponding fit of the electrical resistivity of thin Ag wires 200 nm hight, as reported in Fig. 5b of a paper by Josell et al. [2]. Following these authors, we assume that the grain spacing is the minimum of the height and width of the wire, that the bulk mean free path is $\lambda = 57$ nm and $\rho_0 = 1.6\ \mu\ \Omega\ cm$. It is seen that a good fit is obtained by taking $p = 0$, $p_{GB} = 0$, and $T_{GB} = 0$.

5 Conclusions We report here a new and explicit formula for the electrical conductivity of a thin wire of rect-

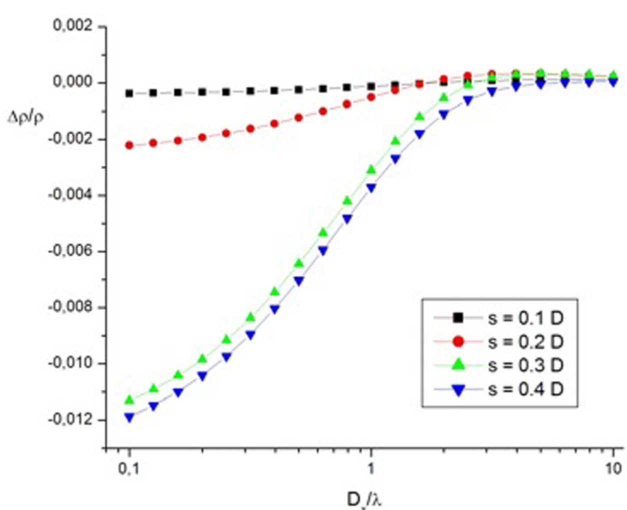

Figure 8 Effect of disorder on the fractional resistivity change of a thin wire of square cross-section with $D_x = D_y = D = 50$ nm. We assume a log–normal distribution of the distances between grain boundaries with mean D and standard deviation s.

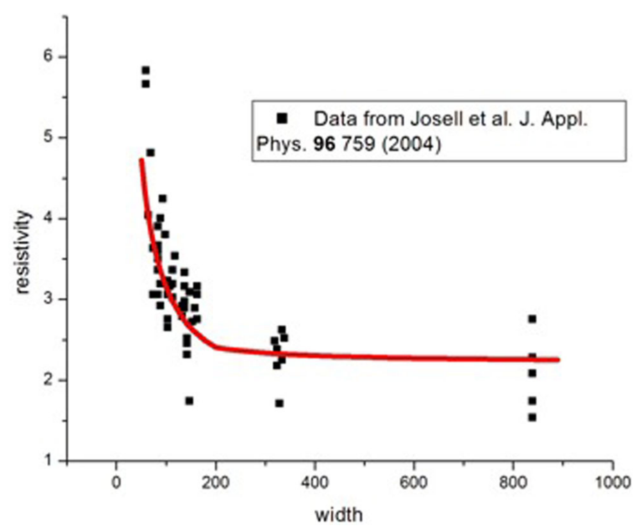

Figure 10 Tentative fit of the theory of this work to data of Josell et al. on the dependence on width of the resistivity of Ag thin wires of rectangular cross-section with height equal to 200 nm. (Fig. 5b of Ref. [2].) $p = 0$; $p_{GB} = 0$; $T_{GB} = 0$; $\rho_0 = 1.6\ \mu\ \Omega$ cm; $\lambda = 57$ nm.

angular cross-section with perfectly diffusive surfaces and in the absence of grain-boundary scattering. The general case, for wires of rectangular or circular cross-section, is further treated by means of the well-known Chambers' method; except that we approximate the exact procedure by summing only over a finite random sample of the infinite number of possible classical trajectories. This can be done to any desired accuracy. Our formulation starts from an exact solution of the Boltzmann transport equation and can treat wires of any width and shape, including the effects of surface roughness and grain boundaries.

As an aside, we have also shown that – except for some exceptional cases – analytical solutions of the Boltzmann equation do not exist for thin wires. This fact throws additional light on the physical significance of the present procedure. Had we performed a summation over the countable infinite set of classical trajectories, as prescribed by the original Chambers' formula, we would have obtained an exact, albeit singular, solution. By summing over a finite number of trajectories we obtain a solution that is regular, but that is only approximate. This can be done within any prescribed accuracy as long as we do not pretend that this accuracy is perfect.

However, it is clear that the lack of existence of the solution of the transport equation is interesting, but not of fundamental importance. This depends on the fact that a transport coefficient obtained from a calculation based on the Boltzmann equation is, in itself, an approximation to a quantum reality that should find its fundament, for instance, in the Kubo formula [6, 7]. If we take the latter type of solution as a starting point and seek its semiclassical form, we find a function in the shape of the corresponding solution of the transport equation, but with perfectly regular analytical properties [8, 21]. Thus, the irregularities of the solution of the Boltzmann equation are only an artifact of this particular approximation, without any counterpart in reality. Accordingly, the proper way to ascertain the significance of the seminumerical procedure we present here is to consider it as an approximation with the same standing as others, whose validity should be gauged independently of them – and that is, perhaps, preferable since it provides answers where others fail to do so.

Acknowledgements The help of J. Moraga-Saez and H. Moreno is gratefully acknowledged. This work was funded in part by project FONDECYT 1120198 and Fondo Interno de Investigación Universidad Central 2013. R. Henriquez acknowledges support from project Conicyt CENAVA 791100037.

Appendix A: The electrical conductivity of a wire of rectangular cross-section in absence of grain-boundary scattering The electrical conductivity of a thin metallic wire of square cross-section and bounded by completely rough surfaces has been calculated by McDonald and Sarginson [10]. Assuming that the applied electric field points in the z-direction, $\mathbf{E} = E\hat{\mathbf{z}}$, that the wire extends from $0 \leq x \leq D_x$, $0 \leq y \leq D_y$ and that it is very long in the z-direction, it is seen that the out-of-equilibrium fraction f_1 of the electronic distribution function satisfies the Boltzmann transport equation (4)

$$v_x \frac{\partial f_1}{\partial x} + v_y \frac{\partial f_1}{\partial y} + \frac{f_1}{\tau} = -eEv_z \left(-\frac{\partial f_0}{\partial \mathcal{E}} \right). \tag{A.1}$$

The solution of this equation can be written in two alternative forms

$$\begin{aligned} f_1 &= -eEv_z \left(-\frac{\partial f_0}{\partial \mathcal{E}} \right) \left[1 - F_x \left(\frac{y}{v_y} - \frac{x}{v_x} \right) e^{-x/\tau v_x} \right] \\ &= -eEv_z \left(-\frac{\partial f_0}{\partial \mathcal{E}} \right) \left[1 - F_y \left(\frac{x}{v_x} - \frac{y}{v_y} \right) e^{-y/\tau v_y} \right], \end{aligned} \tag{A.2}$$

where F_x and F_y are two arbitrary functions of the arguments shown. The only reasonable boundary condition for which it is possible to determine these functions is that of completely diffuse surface scattering; prescribing that f_1 vanishes at $x = 0$, $x = D_y$, $y = 0$, and $y = D_y$. Thus, F_x and F_y have to be such that the solution has the form

$$f_1 = -eEv_z \left(-\frac{\partial f_0}{\partial \mathcal{E}} \right) \left(1 - e^{-d/\lambda} \right); \tag{A.3}$$

where λ is the mean free path and d is the distance – measured along the direction fixed by the velocity v_x, v_y, v_z – between an internal point with coordinates x, y, z and the nearest boundary.

Thus, the average electric current j, flowing in the z-direction, is

$$\begin{aligned} j &= -\frac{2e}{D_x D_y} \left(\frac{m}{2\pi\hbar} \right)^3 \int_0^{D_x} \mathrm{d}x \int_0^{D_y} \mathrm{d}y \int v_z f_1 \mathrm{d}^3\mathbf{v} \\ &= \frac{3\sigma_0}{4\pi D_x D_y} E \int_0^{\pi} \mathrm{d}\theta \cos^2\theta \sin\theta \\ &\quad \times \int_0^{2\pi} \mathrm{d}\phi \left[\int_0^{D_x} \mathrm{d}x \int_0^{D_y} \mathrm{d}y \left(1 - e^{-d/\lambda} \right) \right]; \end{aligned} \tag{A.4}$$

where $v_x = v \sin\theta \cos\phi$, $v_y = v \sin\theta \sin\phi$ and $v_z = v \cos\theta$. Here, σ_0 denotes the electrical conductivity of the bulk material, and

$$\sigma_0 = \frac{\mathcal{N} e^2 \lambda}{m v_\mathrm{F}}; \quad \text{with} \quad \mathcal{N} = \frac{8\pi}{3} \left(\frac{m v_\mathrm{F}}{2\pi\hbar} \right)^3. \tag{A.5}$$

The electrical conductivity σ of the thin wire is defined by Ohm's law $j = \sigma E$; that is

$$\begin{aligned} \frac{\sigma}{\sigma_0} &= 1 - \frac{3}{4\pi D_x D_y} \int_0^{\pi} \mathrm{d}\theta \cos^2\theta \sin\theta \\ &\quad \times \int_0^{2\pi} \mathrm{d}\phi \left[\int_0^{D_x} \mathrm{d}x \int_0^{D_y} \mathrm{d}y e^{-d/\lambda} \right]. \end{aligned} \tag{A.6}$$

Without losing generality we can suppose that $D_x \geq D_y$, so that the aspect ratio is $\mu = D_y/D_x$. On the other hand, we note that the possible values of the distance traversed d are

$$d = \begin{cases} -x/\hat{v}_x; \\ (D_x - x)/\hat{v}_x; \\ -y/\hat{v}_y; \\ (D_y - y)/\hat{v}_y, \end{cases} \tag{A.7}$$

where $\hat{v}_x = \sin\theta\cos\phi$, $\hat{v}_y = \sin\theta\sin\phi$ are components of a unit vector pointing in the direction of the velocity. In fact, the value of d as a function of x, y is the least non-negative quantity of those appearing in the right-hand side of Eq. (A.7). Thus, the integrals over x and y are computable by hand, with the result

$$\frac{1}{D_x D_y}\int_0^{D_x} \mathrm{d}x \int_0^{D_y} e^{-d/\lambda}\mathrm{d}y$$

$$= \begin{cases} \lambda\left[\left|\frac{\hat{v}_x}{D_x}\right| + \left|\frac{\hat{v}_y}{D_y}\right| - 2\lambda\left|\frac{\hat{v}_x}{D_x}\right|\left|\frac{\hat{v}_y}{D_y}\right| \right. \\ \quad \left. + E_x\left(-\left|\frac{\hat{v}_x}{D_x}\right| + \left|\frac{\hat{v}_y}{D_y}\right| + 2\lambda\left|\frac{\hat{v}_x}{D_x}\right|\left|\frac{\hat{v}_y}{D_y}\right|\right)\right] \\ \text{if } |\hat{v}_y|/|\hat{v}_x| < D_y/D_x = \mu; \\ \lambda\left[\left|\frac{\hat{v}_x}{D_x}\right| + \left|\frac{\hat{v}_y}{D_y}\right| - 2\lambda\left|\frac{\hat{v}_x}{D_x}\right|\left|\frac{\hat{v}_y}{D_y}\right| \right. \\ \quad \left. + E_y\left(\left|\frac{\hat{v}_x}{D_x}\right| - \left|\frac{\hat{v}_y}{D_y}\right| + 2\lambda\left|\frac{\hat{v}_x}{D_x}\right|\left|\frac{\hat{v}_y}{D_y}\right|\right)\right] \\ \text{if } |\hat{v}_y|/|\hat{v}_x| > D_y/D_x = \mu; \end{cases}$$

where

$$E_x = \exp\left(-\frac{D_x}{\lambda|\hat{v}_x|}\right), \quad E_y = \exp\left(-\frac{D_y}{\lambda|\hat{v}_y|}\right). \tag{A.8}$$

In consequence, the electrical conductivity is

$$\begin{aligned} \frac{\sigma}{\sigma_0} = 1 - \frac{6\lambda}{\pi}\int_0^{\pi/2} \mathrm{d}\theta\cos^2\theta\sin^2\theta \\ \times\left\{\int_0^{\phi_c}\mathrm{d}\phi\left[\frac{\cos\phi}{D_x} + \frac{\sin\phi}{D_y} - 2\lambda\frac{\cos\phi}{D_x}\frac{\sin\phi}{D_y}\sin\theta\right.\right. \\ \left. + E_x\left(-\frac{\cos\phi}{D_x} + \frac{\sin\phi}{D_y} + 2\lambda\frac{\cos\phi}{D_x}\frac{\sin\phi}{D_y}\sin\theta\right)\right] \\ + \int_{\phi_c}^{\pi/2}\mathrm{d}\phi\left[\frac{\cos\phi}{D_x} + \frac{\sin\phi}{D_y} - 2\lambda\frac{\cos\phi}{D_x}\frac{\sin\phi}{D_y}\sin\theta\right. \\ \left.\left. + E_y\left(\frac{\cos\phi}{D_x} - \frac{\sin\phi}{D_y} + 2\lambda\frac{\cos\phi}{D_x}\frac{\sin\phi}{D_y}\sin\theta\right)\right]\right\}; \end{aligned} \tag{A.9}$$

with $\tan\phi_c = \mu$. Some of the integrals over the angles are elementary and can be performed analytically. By a final change of variable from ϕ to $(1/2)\pi - \phi$ in the last integral, we obtain Eq. (2).

It is found that the direct numerical integration of Eq. (2) is unstable at small values of the aspect ratio. Thus, it is preferable to calculate the electrical conductivity of thin wires of rectangular cross-sections in terms of the functions $\tilde{K}i_n$ defined by

$$\tilde{K}i_n(x) = \int_1^\infty \sqrt{u^2 - 1}e^{-xu}\frac{du}{u^n}; \quad (\Re e\ x > 0). \tag{A.10}$$

This function is a repeated integral of the modified Bessel function $K_1(x)$ [22]

$$\tilde{K}i_1(x) = \int_x^\infty \frac{K_1(t)}{t}\mathrm{d}t; \tag{A.11}$$

$$\tilde{K}i_n(x) = \int_x^\infty \tilde{K}i_{n-1}(x)\mathrm{d}t; \quad (n = 2, 3\cdots). \tag{A.12}$$

The formula for the electrical conductivity is

$$\begin{aligned} \frac{\sigma}{\sigma_0} = 1 - \frac{3\lambda}{8}\left(\frac{1}{D_x} + \frac{1}{D_y}\right) + \frac{4\lambda^2}{5\pi D_x D_y} - \frac{6\lambda}{\pi} \\ \times\left\{\int_0^{\phi_c}\left[\left(-\frac{\cos\phi}{D_x} + \frac{\sin\phi}{D_y}\right)\tilde{K}i_5\left(\frac{D_x}{\lambda\cos\phi}\right)\right.\right. \\ \left. + 2\lambda\frac{\cos\phi}{D_x}\frac{\sin\phi}{D_y}\tilde{K}i_6\left(\frac{D_x}{\lambda\cos\phi}\right)\right]\mathrm{d}\phi \\ + \int_0^{\pi/2-\phi_c}\left[\left(\frac{\sin\phi}{D_x} - \frac{\cos\phi}{D_y}\right)\tilde{K}i_5\left(\frac{D_y}{\lambda\cos\phi}\right)\right. \\ \left.\left. + 2\lambda\frac{\cos\phi}{D_x}\frac{\sin\phi}{D_y}\tilde{K}i_6\left(\frac{D_y}{\lambda\cos\phi}\right)\right]\mathrm{d}\phi\right\}. \end{aligned} \tag{A.13}$$

These functions can be explicitly calculated by using the formulae

$$\begin{aligned} \tilde{K}i_6(x) = \frac{1}{120}\left[(x^5 - 10x^3 - 15x)Ki_1(x)\right. \\ \left. - (x^5 - 9x^3 - 16x)K_1(x) + (x^4 - 7x^2)K_0(x)\right]; \\ \tilde{K}i_5(x) = \frac{1}{24}\left[-(x^4 - 6x^2 - 3)Ki_1(x)\right. \\ \left. + (x^4 - 5x^2)K_1(x) - (x^3 - 3x)K_0(x)\right]; \end{aligned} \tag{A.14}$$

in terms of the modified Bessel functions $K_0(x)$ and $K_1(x)$ and the Bickley (or Bickley–Naylor) function [22]

$$Ki_1(x) = \int_x^\infty K_0(t)\mathrm{d}t. \tag{A.15}$$

A copy of a program (in FORTRAN) that returns the value of electrical conductivity, as given by Eq. (A.13), may be obtained from the corresponding author.

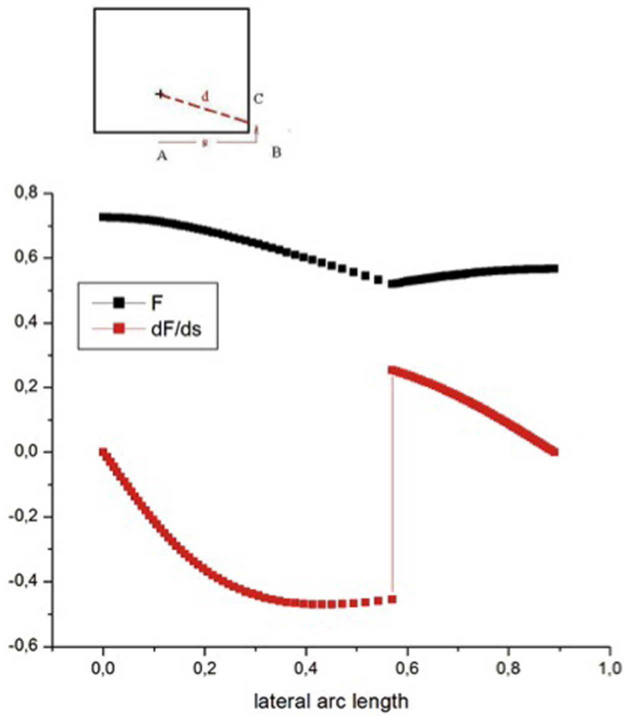

Figure 11 In a neighborhood of a corner of the enclosure the characteristic F function is continuous (with the shape of an inverted cusp) while its derivative with respect to the lateral arc length s has a finite discontinuity.

Appendix B: Solution of the Boltzmann equation for partially diffuse surface scattering In this appendix we investigate in detail the way in which the solution of the Boltzmann transport equation (4) exists for the case $p = 0$; but fails to do so when $p \neq 0$.

In the completely diffuse case $p = 0$, the characteristic function is $Fe^{-t/\tau} = e^{-d/\lambda}$, where d is the distance to the nearest boundary point. This is illustrated in the insert in Fig. 11

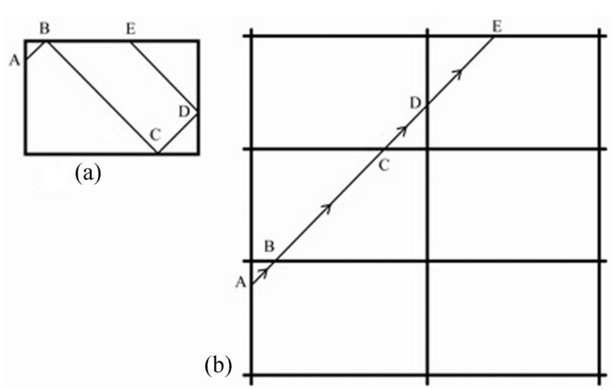

Figure 12 (a) Inside a partially reflecting enclosure (section of a grain or of a thin wire of rectangular cross-section) the path of a carrier may be subject to multiple reflections (Fig. 8 of Josell et al. [2]). (b) In a repeated section schema, the trajectory appears as a straight line. If prolonged long enough, the line will pass arbitrarily near some corner.

for a given point internal to a thin wire of rectangular cross-section – or, alternatively, a point inside a grain limited by perfectly diffuse grain boundaries. If we plot $e^{-d/\lambda}$ as a function of the lateral arc length s, we note that it has the shape of an inverted cusp in the neighborhood of each point where the boundary suddenly changes its direction. Near each of these corner points, the characteristic function is continuous, but its derivative with respect to s has a finite discontinuity.

In the case $p = 0$ and for a given internal point, these singularities are isolated and constitute a set of measure zero. But the situation is radically changed when $p \neq 0$. As shown in Fig. 12a, trajectories with repeated reflections at the boundaries are then possible. It is useful to plot the same trajectory in a repeated section schema. As shown in part (b) of the same figure, the trajectory is now a straight line. It is obvious (except for the isolated cases of perfectly horizontal or vertical directions) that – if this line is prolonged long enough – it will pass arbitrarily near one of the repeated images of the corner points. Since the characteristic function contains in this case trajectories of all lengths, it is seen that it will have a cusp-like singularity in each direction. Thus, we conclude that, when $p \neq 0$, the characteristic function (and, thus, the solution of the Boltzmann transport equation) is continuous with discontinuous derivatives for almost every value of $\hat{\mathbf{v}}$.

References

[1] W. Steinhögl, G. Schlinder, G. Steinlesberger, and M. Egelhardt, Phys. Rev. B **66**, 075414 (2002).
[2] D. Josell, C. Burkhard, Y. Li, Y.-W. Cheng, R. R. Keller, C. A. Witt, D. R. Kelley, J. E. Bonevich, B. C. Baker, and T. P. Moffat, J. Appl. Phys. **96**, 759 (2004).
[3] W. Steinhögl, G. Schlinder, G. Steinlesberger, M. Traving, and M. Egelhardt, J. Appl. Phys. **97**, 023706 (2005).
[4] A. Bid, A. Bora, and A. K. Raychaudhuri, Phys. Rev. B **74**, 035426 (2006).
[5] R. L. Graham, G. B. Alers, T. Mountsier, N. Shamma, S. Dhuey, S. Cabrini, R. H. Geiss, D. T. Read, and S. Peddeti, Appl. Phys. Lett. **96**, 042116 (2010).
[6] D. A. Greenwood, Proc. Phys. Soc. Lond. **71**, 585 (1958).
[7] R. Kubo, J. Phys. Soc. Jpn. **12**, 570 (1957).
[8] L. Sheng, D. Y. Xing, Z. D. Wang, and J. Dong, Z. Phys. B **100**, 567 (1996).
[9] R. B. Dingle, Proc. R. Soc. A **201**, 545 (1950).
[10] D. K. C. McDonald and K. Sarginson, Proc. R. Soc. A **203**, 233 (1950).
[11] J. R. Sambles, K. C. Elsom, and T. W. Preist, J. Phys. F **12** 1169 (1982).
[12] K. Fuchs, Proc. Camb. Philos. Soc. **34**, 100 (1938).
[13] A. F. Mayadas, M. Shatzkes, and J. F. Janak, Appl. Phys. Lett. **14**, 345 (1964);
A. F. Mayadas and M. Shatzkes, Phys. Rev. **1**, 1382 (1970).
[14] J. Szczyrbowski and K. Schmalzbauer, J. Phys. F **16**, 2079 (1986).
[15] R. Dimmich and F. Warkusz, Active Passive Electron. Compon. **12**, 103 (1986).
[16] R. G. Chambers, Proc. Phys. Soc. A **65**, 458 (1952); Proc. Phys. Soc. A **238**, 344 (1957).

[17] R. Courant and D. Hilbert, Methods of Mathematical Physics II (Interscience, New York, 1962), chap. 2.
The method can be used even when the relaxation time approximation cannot be invoked, see: K. K. Thornber, Applications of path integrals to problems in dissipation, in: Path Integrals and their Applications in Quantum, Statistical, and Solid State Physics, edited by G. J. Papadopoulos and J. T. Devreese (Plenum Press, New York, 1978), pp. 359–382.
[18] J. M. Ziman, Principles of the Theory of Solids (Cambridge University Press, London, 1972), p. 213.
Instead of the wave vector $\mathbf{k}$ we use the velocity $\mathbf{v}$, according to $\hbar\mathbf{k} = m\mathbf{v}$.
[19] In a more exact treatment, this number is replaced by a function depending on the angle of incidence, see: J. M. Ziman, Electrons and Phonons (Clarendon Press, London, 1962), pp. 456–460.
[20] J. P. Golledge, T. W. Preist, and J. R. Sambles, J. Phys. F **17**, 1411 (1987).
[21] L. Sheng, D. Y. Xing, and Z. D. Wang, Phys. Rev. B **51**, 7325 (1995).
[22] Y. L. Luke, Integrals of Bessel Functions (McGraw-Hill, New York, 1962);
M. Abramowitz and I. A. Stegun, Handbook of Mathematical Functions (Dover Publications, Inc., New York, 1972), pp. 479–494.